Mechanically tunable multiphoton fabricated protein hydrogels investigated using atomic force microscopy†

Constantine Y. Khripin,[a] C. Jeffrey Brinker[abc] and Bryan Kaehr*[c]

Received 19th January 2010, Accepted 15th April 2010
First published as an Advance Article on the web 11th May 2010
DOI: 10.1039/c001193b

Recent work has demonstrated the feasibility of employing three dimensional (3D) protein hydrogels, fabricated using multiphoton-induced photochemistry, as chemically responsive microactuators in "lab on a chip" devices. In addition, these materials show great promise as cell capture/incubation devices, allowing single bacterial cells to reproduce into multicellular constructs with "user-defined" 3D geometries. However, to date, the mechanical properties of these materials, critical for these applications, have not been quantitatively characterized. In this work, we develop and apply a method to measure the elastic modulus of microfabricated protein hydrogels *in situ* under dynamic physical and chemical environments. We fabricated protein microcantilevers using a wide range of protein building blocks (albumin, lysozyme, avidin) and probed their mechanical properties using atomic force microscopy (AFM). The length dependence of the spring constant displayed by protein cantilevers followed the predicted cantilever model, yielding the elastic modulus of the material. By varying laser dwell time, the modulus of protein cantilevers could be tuned over 2 orders of magnitude (from 0.03 to 3 MPa for albumin), a range that encompasses modulus values for a number of biological tissues (*e.g.*, cartilage, basement membrane). Further, the modulus was shown to vary strongly over a range of pH values (pH 2–12). Distinct profiles of pH *vs.* modulus for albumin, lysozyme and avidin cantilevers were observed, which correlate to structural transitions of the incorporated protein. Modification of protein cantilevers *via* ligand binding (biotin to avidin), increased cantilever stiffness. Finally, using the modulus of a hydrogel microchamber calculated *in situ*, we determined the pressure generated by a replicating bacterial colony entrapped in the microchamber to be 2.7 ± 1.3 kPa. This work demonstrates an ability to quantify mechanical properties under both chemically and biologically dynamic microenvironments and will enable the development of a robust platform to investigate cell/microenvironmental interactions with high spatial resolution, in three dimensions, using mechanically tunable biological materials.

Introduction

The chemical and physical interactions with the surrounding microenvironment encountered by developing cells play a crucial role in determining cell fate. For instance, it is increasingly evident under *in vitro* cell culture conditions that the elasticity of the substrate can alter the outcome of cell development for a wide range of cell types.[1–5] Although the bulk mechanical properties of native biological tissues such as cartilage[6–8] have been well studied, there is a strong interest in determining microscale properties of biological tissues with the potential to model these properties *in vitro*.[9–11] Thus, in addition to biocompatibility and chemical functionality, *in vitro* cell culture substrates should be capable of mirroring the mechanical properties of the biogenic tissue microenvironments they are intended to represent—potentially in three dimensions—in order to successfully replicate *in vivo* development.

Consequently, microtechnologies have been increasingly employed to fabricate cell substrates of ever more complexity and greater environmental control.[12,13] Of these strategies, multiphoton fabrication[14] shows enormous promise to provide true 3D control over the physical and chemical microenvironment. Multiphoton fabrication is an inherently 3D direct-write method reliant on non-linear photoexcitation to induce chemistry (*e.g.*, photo-crosslinking[15]) in highly resolved 3D reaction volumes. Recently, this strategy has been applied to the fabrication of biocompatible protein hydrogels with arbitrary 3D shape.[16–19] Many applications for employing these materials for cellular studies have been explored, including chemical and topographical guides to direct neuronal growth[15,20] and containment devices to direct the position and motion of motile bacteria.[16–18] These structures offer enormous opportunity to study the behaviour and development of isolated cells and cell populations using well-defined 3D geometries. However, the mechanical properties of this promising class of materials have not been quantitatively characterized. In addition, the complex

[a]*Center for Micro-Engineered Materials, University of New Mexico, Albuquerque, NM, USA*
[b]*Departments of Chemical and Nuclear Engineering and Molecular Genetics and Microbiology, University of New Mexico, NM, USA*
[c]*Sandia National Laboratories, Advanced Materials Lab, NM, 87106, USA. E-mail: bjkaehr@sandia.gov; Fax: +1 505-272-7336; Tel: +1 505-272-7665*

† Electronic supplementary information (ESI) available: Plots of spring constant as a function of length for several albumin, avidin and lysozyme cantilevers. See DOI: 10.1039/c001193b

chemical and physical dynamics of cellular microenvironments requires the development of *in situ* analytical methodologies in order to understand and ultimately tune cell/material interactions. In this work, we undertake a quantitative study of the mechanical properties of multiphoton fabricated protein hydrogels in dynamic aqueous environments, and develop a methodology to assess cell/material interactions *in situ*.

The mechanical properties of proteinaceous materials vary greatly, from hundreds of Pa for some hydrogels such as Matrigel™[10] and fibrinogen composites[11] to several GPa for some protein fibres and silk.[21] It has been shown that the properties of multiphoton fabricated protein hydrogels depend strongly on processing parameters and conditions in the medium.[17] For example, protein hydrogels expand and contract depending on the pH of the medium, with the greatest degree of contraction occurring at the pH near the isoelectric point of the constituent protein,[17] a property which has been exploited to drive concerted and independent microactuation schemes following changes to the chemical medium.[17] This strongly suggests that the properties of the hydrogel depend directly on the properties of individual proteins incorporated into the matrix. Careful selection of constituent proteins, fabrication parameters (*e.g.*, laser irradiance), and fluidic medium should enable the mechanical properties of protein hydrogels to be highly tunable, offering unique opportunities to control the behaviour of developing cells in three dimensions.

In previous work, the modulus of hydrogels was measured using bulk techniques[11,22] as well as microindentation with a spherical tip.[9,10] However, the former method cannot be applied to microstructures, and the latter requires that the microstructures be large compared to the indenter, the size of the indenter be matched to sample modulus, and assumptions be made with regards to Poisson's ratio and indenter shape. To address these issues, herein we describe a method for *in situ* measurement of the elastic properties of protein hydrogel microstructures. 3D cantilevered beam structures comprised of photo-crosslinked proteins were fabricated using multiphoton fabrication. The deflection of the mathematically straightforward cantilevers, measured in liquid using an atomic force microscope (AFM), was used to determine the material modulus.

First, we demonstrate that the protein cantilevers follow the standard cantilever beam model. We then examine how the modulus of the hydrogel varies with the fabrication conditions, the pH and temperature of the medium, and how it can be altered following ligand binding to constituent protein monomers. Finally, we examine the interaction of these materials with developing cells by confining a replicating bacterial colony in a protein chamber. The extent of chamber deformation induced *via* cell growth, together with an *in situ* measurement of protein hydrogel elastic modulus, is used to calculate the pressure exerted by the bacterial colony.

Experimental methods

Fabrication of microstructures

Microstructures composed of photo-crosslinked protein were fabricated from solutions containing protein at 320 mg ml^{-1} (unless otherwise specified) and methylene blue (4 mM) as a photosensitizer. Microstructure geometries were defined using a mask-directed multiphoton lithography approach previously described in detail.[16,19] Briefly, cantilevers composed of photo-crosslinked protein were fabricated onto untreated no. 1 microscope cover slips by using the output of a mode-locked titanium : sapphire laser (Tsunami; Spectra Physics) operating at 730–740 nm. In some instances, the cover glass was boosted ~40 μm over a lower cover glass by using microspheres. The laser focus was raster scanned with an X/Y open frame scan head (Nutfield Technology) across a reflectance mask (digital micromirror device) used to define the features of protein microstructures as the laser focus was stepped axially from the substrate. The laser output was adjusted by using optics to approximately fill the back aperture of an oil-immersion objective (Nikon 100× Fluar, 1.3 numerical aperture) situated on a Nikon inverted microscope. Laser power, obtained by attenuating the laser beam using a half-wave plate/polarizing beam-splitter pair, was approximately 30 mW at the objective unless otherwise specified. Laser dwell time during fabrication was modified by changing the frequency of the X-component of the raster scan (ranging from 0.1–0.01 Hz; the *Y* frequency was kept constant at 180 Hz for all experiments).

Atomic Force Microscopy (AFM) measurements

AFM measurements of cantilever stiffness were carried out using the MFP3D-Bio AFM (Asylum Research, Santa Barbara, CA) mounted on an inverted Nikon TE2000U microscope. Two commercial tip-less AFM cantilevers were used in this study (Arrow-TL1, $k = 0.03$ N m^{-1}, TL-FM, $k = 2.6$ N m^{-1} from Nanoworld AG, Switzerland). Cantilevers were kept in liquid media for all AFM measurements. The AFM cantilever was positioned over the microstructure using a combination of manual positioning and the automated AFM XY stage while monitoring structures visually using a 30× objective.

Microcantilever length and width were measured optically using the inverted microscope. The thickness was measured either destructively, by removing the microcantilever and imaging it with AFM, or by fabricating the protein cantilever close to the glass cover slip and pressing it with the AFM cantilever until it made contact with the substrate, enabling the thickness to be determined.

The buffer used for the pH dependence study was 10 mM sodium chloride, 0.5 mM sodium tetraborate, 0.5 mM sodium phosphate monobasic, and 0.5 mM sodium citrate monobasic with pH adjusted using HCl and NaOH. This mixture ensured sufficient buffering over the range of pH from 2 to 11. Data points shown in Fig. 3 were normalized using the modulus value of the cantilever recorded at pH 7; values measured for 9 protein cantilevers were: albumin, 0.95, 3 MPa; lysozyme 4.0, 4.5, 3.0, 7.0, and 7.0 MPa; avidin 0.6, 1.2 MPa. Biotin binding to avidin microstructures was accomplished by incubating structures in 1 mM biotin in phosphate buffered saline (PBS) for 30 minutes. All other studies were carried out in phosphate buffered saline (PBS) free of divalent cations. The temperature dependence study was carried out using a heated liquid cell (Asylum Research, Santa Barbara, CA). All reagents were obtained from standard sources.

Imaging of the bacterial chamber was carried out in liquid using tapping mode AFM. Triangular cantilevers with an oxide

sharpened pyramidal point (TR400PB, $k = 0.09$ N m^{-1}, made by Olympus, obtained from Asylum Research) were used for imaging and for probing the hydrogel cantilever.

Scanning Electron Microscopy (SEM)

Protein microstructures were fixed in 2.5% glutaraldehyde solution for 20 min, dehydrated by using 10 min sequential washes [2 : 1 ethanol/H_2O; twice in 100% ethanol; 1 : 1 ethanol/methanol; 100% methanol; all solutions stated as vol/vol; allowed to air dry for 3 h, and sputter-coated to nominal thicknesses of 10 nm with Au. Images were recorded using an FEI Quanta series scanning electron microscope.

Bacterial cell culture

E. coli strain RP9535 (smooth-swimming, ΔcheA; kindly provided by J. S. Parkinson, U of Utah) were grown aerobically in tryptone broth (TB) at 37 °C and harvested at mid-logarithmic phase. Cells were diluted 100-fold into PBS (pH 7.0) and introduced into 35 mm cover slip-bottom dishes containing microchambers fabricated onto the glass substrate. Trapped cells were incubated for ~12 to 24 hours in TB (37 °C).

Results and discussion

Fabricated microcantilevers (Fig. 1A) consist of a narrow beam extending from a block anchored to the substrate. This cantilever beam configuration has a spring constant k given by[23]

$$k = \frac{Ewt^3}{4l^3} \quad (1)$$

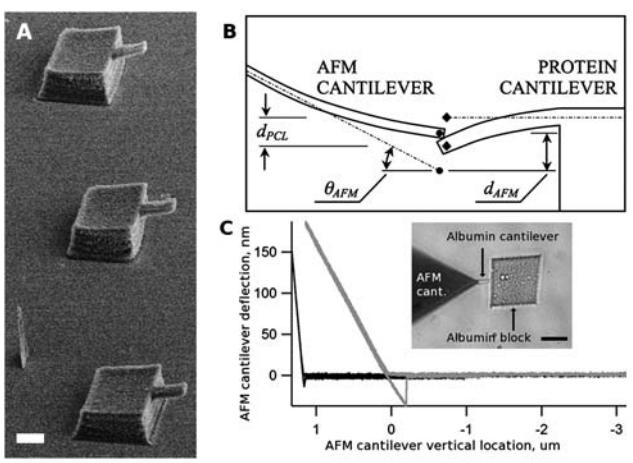

Fig. 1 Multiphoton fabricated protein microcantilevers investigated using AFM. Protein microcantilevers (A, SEM image, scale bar, 5 μm) are tested in aqueous media by pressing with an AFM cantilever (B). An AFM force curve with the recorded cantilever deflection on the ordinate and the AFM z position on the abscissa is shown in C. The black force curve was collected by pressing the AFM tip on the glass substrate, and consequently the slope = 1. The grey curve was collected by pressing the AFM tip upon the tip of the protein microcantilever (inset) and the slope < 1 due to the additional compliance of the protein microcantilever. The inset shows an optical microscope image of the AFM cantilever (dark triangle) positioned at the tip of a protein cantilever (scale bar, 10 μm).

where E is the modulus, w the width, t beam thickness and l beam length. The advantage of using a cantilever beam to determine the modulus of the material is that the spring constant k is linear with E, and Poisson's ratio need not be known. This method has been used to characterize the modulus of microcantilevers made from polymer mixtures using multiphoton polymerization.[24] In order to determine k, we apply a force to the protein cantilever by pressing with a tipless AFM cantilever (Fig. 1B). Both cantilevers deflect as a result of the interaction, by distance d_{AFM} for the AFM cantilever and d_{PCL} for the protein cantilever. Applying a force balance, we find that the spring constant of the protein cantilever, k_{PCL}, is given by

$$k_{PCL} = \frac{k_{AFM} d_{AFM}}{d_T - d_{AFM}} \quad (2)$$

where k_{AFM} is the known spring constant of the AFM cantilever. The quantities $d_T = d_{PCL} + d_{AFM}$ and d_{AFM} are measured by the AFM instrument. During a measurement, the AFM cantilever is positioned over the tip of the protein cantilever using a piezoelectric XY stage. AFM cantilever deflection is recorded while the cantilever is lowered to press the protein cantilever and retracted. A typical force curve is shown in Fig. 1C along with an optical image of AFM probe positioning (inset).

The spring constant of protein microcantilevers, calculated from AFM data using eqn (2), followed eqn (1) with respect to cantilever length (see ESI, Fig. S1†). This confirms that the microcantilever spring constant can be used to calculate the material modulus using eqn (1), as has been shown in previous work.[24]

Elastic modulus of protein hydrogels

The elastic modulus of two sets of albumin microcantilevers, measured at pH 7 in PBS is plotted in Fig. 2 as a function of laser dwell time. The stiffness of the hydrogel increases with laser dwell time, a fabrication parameter that increases the density/degree of crosslinking of the protein hydrogel.[17] Here, eqn (1) was used to calculate the modulus of the protein hydrogel from cantilever spring constants. The error bars represent the standard deviation of 3 measurements; high reproducibility is demonstrated by the two sets of cantilevers. The capability to tune hydrogel modulus

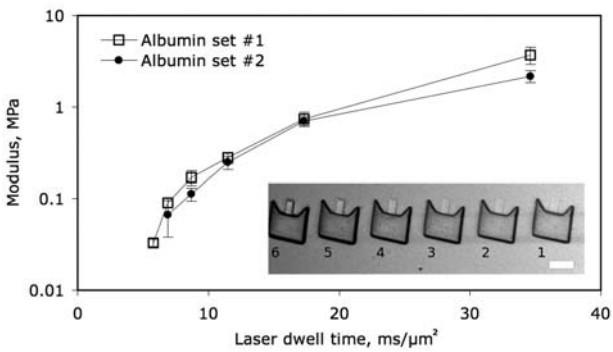

Fig. 2 The modulus of albumin hydrogels as a function of laser dwell time shows tunability over two orders of magnitude. The two sets of structures shown here were prepared and measured in separate experiments. Set #1 is shown in the inset (scale bar 10 μm) with structures 1–6 corresponding to data points 1–6 (left to right).

using this approach did not depend on the identity of the incorporated protein, and we obtained modulus values over a range of 0.6–9 MPa for lysozyme, and 0.2–12 MPa for avidin hydrogel cantilevers.

Toward employing multiphoton fabricated protein hydrogels for cell scaffolding/tissue engineering, it is useful to compare these modulus values to what has been reported for native biological structures. Considering biological tissue, the modulus of cartilage has been reported at 3–30 MPa,[6] 0.47–0.9 MPa,[8] and 2–40 MPa[7] for various tissue sources. This variation can be attributed to natural variations in tissue[6] as well as to the viscoelastic nature of cartilage that makes accurate measurements and comparisons problematic.[7] This differs from the protein hydrogels examined here, which showed no dependence of modulus on the rate of cantilever bending over the (AFM-tip) velocity range of 0.1–4.0 μm s^{-1}. The modulus of another important extracellular structure, the basement membrane, has been recently measured to be 10–50 kPa.[9] By comparison, the modulus of Matrigel™ has been measured to be 400–800 Pa,[10] and that of fibrinogen composites to be 20 Pa–8 KPa.[11] As has been observed by other workers,[10] these synthetic materials appear to be much softer than native biological scaffolds. Nonetheless, the range of moduli demonstrated here for multiphoton fabricated protein hydrogels (0.03 MPa to ~3 MPa) readily accommodates a significant portion of measured modulus values for both native and artificial biological scaffolds, indicating the feasibility to employ these materials as mechanically tunable 3D substrates presented to cells.

Modulus variation with pH and temperature

The pH of the medium can influence strongly the structure of a protein. Significant deviation from the isoelectric point (pI) incurs excess charge that can destabilize and ultimately unfold the protein,[25,26] causing multiphoton fabricated protein hydrogels to swell at values outside the pH of the isoelectric point of the constituent protein.[17] We investigated the pH-dependent modulus using cantilevers comprised of albumin, avidin, and lysozyme. In all, 5 lysozyme cantilevers, 2 albumin cantilevers and 2 avidin cantilevers were tested for pH dependence. Fig. 3 shows that the elastic modulus is greatest at pH ≈ pI (reported pI of 4.7–4.9 for albumin, 10–10.5 for avidin, and 11–11.3 for lysozyme[27,28]). Here, the error bars indicate a 95% confidence interval in the average value derived from multiple tests performed on multiple structures.

There has been substantial work investigating structural properties of albumin as a function of pH. At pH 3.4–4.4, the albumin molecule undergoes the natural state to expanded state (N–E) transition, a reversible change characterized by expansion, isomerization and a helix–coil transition.[29,30] At pH 7–9, the natural–basic state (N–B) transition takes place.[31] We observe that the modulus of albumin microcantilevers undergoes significant changes at these pH values indicating that structural transformations of constituent albumin are retained in the protein hydrogel. Further, thermal denaturation experiments are in qualitative agreement with our observations for albumin cantilevers, with greatest protein stability—and cantilever stiffness—occurring in the pH 5–7 range.‡ However, we do not detect a strong effect on the elastic modulus following acidic (<pH 3) and alkaline (>pH 10) swelling.[17,31]

Less information is available on how the structure of avidin and lysozyme change with pH. At room temperature, lysozyme undergoes no significant structural changes over the entire range of pH 2–11. However, lysozyme has been shown to be progressively more susceptible to thermal denaturation below pH 5,[32,33] and there is spectroscopic evidence of disruption of stabilizing tryptophan–COOH bonds below pH 7.[32] We observe a substantial decrease in the modulus of lysozyme hydrogel cantilevers below pH 6, suggesting that these structural changes influence the mechanical properties of lysozyme hydrogels. Avidin is known to be very stable over the pH range 2–11;[34] nevertheless we observe a strong dependence of modulus on pH. Thus the dynamic response of elastic modulus over pH 2–11 observed for the avidin hydrogels may be indicative of subtle structural

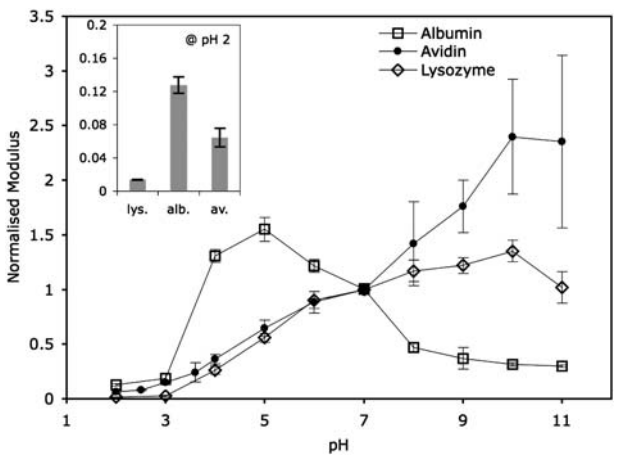

Fig. 3 Elastic modulus of protein microcantilevers as a function of pH. The elastic modulus was normalised to the modulus measured at pH 7. The inset compares the normalized modulus at pH 2.

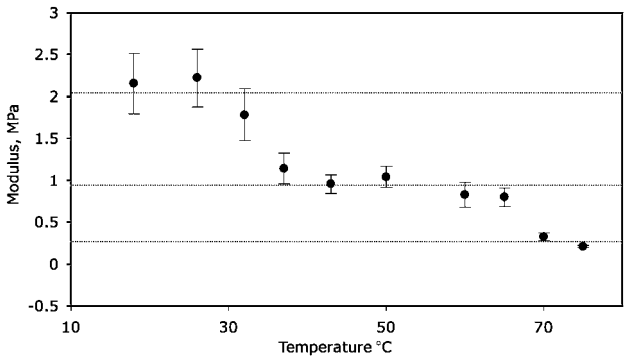

Fig. 4 The modulus of an albumin protein cantilever as a function of temperature. The dotted lines are intended as guides for the eye.

‡ Our data are also in agreement with information on albumin hydrophobicity. The hydrophobicity of a protein can be measured by deuteration experiments that measure the number of hydrogens accessible to deuterium exchange. For albumin, the number of inaccessible protons is greatest at pH 5, decreases rapidly at pH < 5 and decreases slowly from pH 5 to pH 8.5.[42] A qualitatively similar pH dependence of modulus is seen in Fig. 3.

changes that may not denature the protein, but otherwise confer greater susceptibility to mechanical deformation.

The stability of protein molecules also depends on temperature. Fig. 4 shows how the modulus of an albumin hydrogel cantilever varies with temperature. Here, we observe that the modulus decreases significantly at two points: 30 °C and 70 °C (error bars are 95% confidence intervals in standard error). For albumin, two denaturation temperatures have been reported.[35,36] The higher denaturation temperature is near 70 °C,[35,37] which is supported by our data. The lower denaturation temperature has been placed at 0 °C[35] and 20 °C[36] with an additional study showing ΔG of denaturation of albumin occurring at 30 °C.[35] We observed a marked decrease in modulus between 26 and 37 °C for albumin cantilevers.

Our observation that the elastic modulus of the protein cantilever changes significantly at the denaturation temperatures reported for albumin supports the conclusion that the mechanical properties of protein hydrogels are tightly linked with the stability of the constituent protein molecules.

Effect of biotin binding on avidin hydrogel modulus

Avidin binds biotin (vitamin B7) with very high affinity. The resulting avidin/biotin complex is more robust, denaturing at a higher temperature[38] compared to apo-avidin.

Deuterium exchange studies have shown that the complex is more compact and hydrophobic in comparison to apo-avidin.[39] Further, swelling of hydrogels comprised of avidin is attenuated significantly in acidic medium following biotin-binding.[17] Given this evidence, we expect that the modulus of avidin hydrogels should increase following the binding of biotin. Fig. 5 compares the elastic modulus of several avidin cantilevers, before and after the addition of biotin, in PBS and in 10 mM HCl.

These measurements were conducted sequentially on four microcantilevers over a range of initial modulus values (0.2–12 MPa; fabricated, lowest to highest, using increasing laser dwell times). First, modulus was measured in PBS. Then the sample was rinsed several times with 10 mM HCl in H_20 and subsequently measured in this rinse solution. Next, the structures were incubated for 30 minutes in 10 mM biotin in PBS. After thorough rinsing in PBS, the modulus measurements were repeated as described above in fresh PBS and HCl solutions.

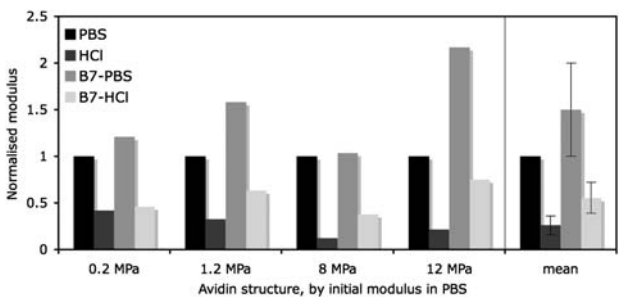

Fig. 5 The modulus of avidin microcantilevers, initially measured in PBS (PBS, black bars) and 10 mM HCl (HCl, dark grey bars), increases significantly in both PBS (B7-PBS, grey bars) and HCl (B7-HCl, light grey bars) solutions after incubation with biotin followed by extensive rinsing. Error bars in the left panel span the 95% confidence interval in the mean value. All values normalized to that of "PBS".

Our data show that the modulus of avidin hydrogels increases significantly both in PBS and in 10 mM HCl, consistent with previous observations of the effect of biotin binding on the structure of avidin outlined above. This ligand-mediated mechanical response of avidin hydrogels to biotin may provide a unique route to autonomously modulate components in cell/microfabricated environments *in situ*.

Measuring the pressure generated by a confined bacterial colony undergoing cell division

In the above analysis, we have established that multiphoton fabricated protein hydrogels can be constructed with prescribed modulus over a range of values spanning those measured for native and artificially derived biological scaffolds. Here, we examine the mechanical interaction between an albumin hydrogel microchamber and a replicating bacterial colony confined within it.

Protein microstructures can be engineered to trap motile bacteria from the surrounding fluidic environment.[16,17,19] Diffusion of nutrients and wastes across protein hydrogel barriers enables trapped bacteria to reproduce inside a chamber. Cell division can lead to the chamber cavity filling with cells and exerting a pressure that can result in deformation of protein chamber walls. This process has been described in detail where large deformations of chamber ceilings were observed.[17]

We designed an experiment to investigate this cell/material interaction using our AFM approach. Here, motile *E. coli* RP9535 were incubated with chambers comprised of albumin and microfabricated with thick side-walls and thin ceilings. Capture of motile cells in microchambers from the environment, followed by incubation in nutrient media, resulted in the cell colony expanding to fill the chamber (Fig. 6A), ultimately leading to deformation of the chamber ceiling (Fig. 6B–D).

The height profile of this deformation was measured by AFM. The elastic modulus of the chamber ceiling was measured *in situ* using microcantilevers that were fabricated simultaneously with the ceiling (Fig. 6B and D). After an AFM image of the chamber was recorded, the AFM probe was used to depress the cantilevers and the modulus was calculated as described above.

The ceiling of the chamber can be viewed as a clamped membrane. Because it is much thinner than it is wide, we can neglect bending and analyze the deformation using a formulation for the centre deflection of a square membrane,[40] d_m,

$$d_m = f(\nu)\left(\frac{P_L a^4(1-\nu)}{Et}\right)^{\frac{1}{3}} \quad (3)$$

where P_L is the pressure inside the chamber, a is the chamber half-width, ν is Poisson's ratio, E is Young's modulus, t is ceiling thickness and $f(\nu)$ can be approximated by $f(\nu) \approx 0.8 + 0.062\nu$. Furthermore, data from a numerical solution of the lateral and diagonal height profiles has been reported.[40] These height profiles, shown in Fig. 6E and F, are in good agreement with the predicted profiles.

Using the ceiling modulus of $E = 0.3 \pm 0.14$ MPa (based on the average of the two cantilevers in Fig. 6B), and the measured dimensions of the chamber, $a = 8$ μm, $t = 1.5$ μm, $d_m = 1.8$ μm,

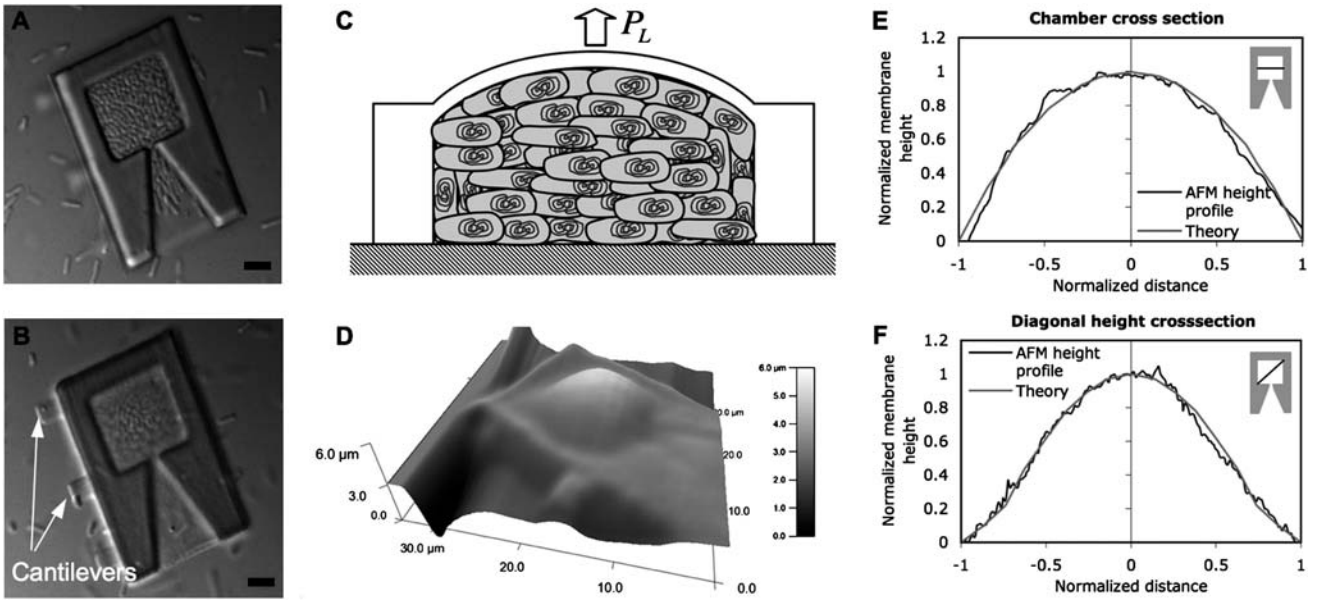

Fig. 6 Motile bacteria are captured from the surrounding environment and confined in a protein microchamber (A and B, images show the glass substrate/chamber interface and the chamber ceiling respectively; scale bars, 10 μm); bacterial cells reproduce, filling the chamber and deforming the chamber ceiling (B–D). The deflection of the membrane, measured by AFM, is compared to a theoretical model for the lateral (E) and diagonal (F) cross-sections. Cantilevers fabricated in conjunction with the ceiling layer are used to measure the modulus of the ceiling material, which in turn is used to calculate the pressure inside the chamber.

and assuming Poisson's ratio (ν) of 0.5 (assumed for a soft hydrogel[10]), we calculate an internal pressure of 2.7 ± 1.3 kPa. This pressure is comparable to the elevated pressure reported for cancer tumors.[41] It also approximately corresponds to a force of 15 nN per bacterium,§ or, on a mass basis, to one person holding up 50 thousand tons.

Conclusions

We demonstrated multiphoton fabrication of protein microcantilevers whose mechanical properties were determined using a cantilever beam model. We have shown that, depending on laser dwell time, which governs the extent of protein crosslinking, the modulus of these cantilevers can be varied over several orders of magnitude, across a range relevant to many types of biological tissues (see Fig. 7). The ability to mimic the modulus of biological microenvironments is crucial towards understanding, and ultimately directing cell fate in artificial (*i.e.*, *in vitro*) settings. Thus, multiphoton fabricated protein microstructures show great potential to serve as a highly tunable platform for studying the interaction of cells with tissue microenvironments.

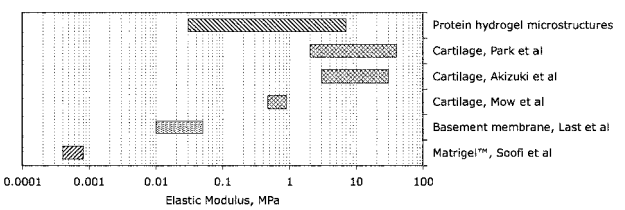

Fig. 7 The modulus of protein microstructures covers a broad range that encompasses biological tissues such as basement membranes and cartilage.

An interesting question raised in this study is how the modulus of protein hydrogels is related to the modulus of constituent proteins. Our observations of protein hydrogel modulus as a function of pH, temperature, and ligand binding correlate well with known structural transitions of the protein molecules. Transitions such as the N–E and N–B transitions of albumin, as well as the compaction avidin undergoes after binding biotin, strongly influence the elastic modulus of the microcantilevers derived from these constituent proteins. Thus, it should be feasible to investigate structural transitions of protein molecules using the system described here—provided the establishment of an appropriate theoretical framework.

Finally, we measured the pressure exerted on a hydrogel membrane of known modulus by a colony of *E. coli* confined in a microchamber. The accuracy of this technique relied on an *in situ* measurement of the modulus of the microchamber roof using cantilevers built into the structure. This preliminary study demonstrates the possibility of using 3D protein hydrogels to create cell/material interfaces with precise mechanical properties and should facilitate development of *in vitro* cell models aimed at understanding cell confinement effects found, for instance, during stages of infection and tumor development.[5]

Acknowledgements

We acknowledge the US Department of Energy, Office of Science, Office of Basic Energy Sciences, Division of Materials Science and Engineering, as well as Air Force Office of Scientific Research grant FA 9550-07-1-0054 for support of this work. BK

§ Force per bacterium was calculated from the chamber pressure and an estimate of the surface area per bacterium (5.5 μm^2).

gratefully acknowledges the Sandia National Laboratories Truman Fellowship in National Security Science and Engineering and the Laboratory Directed Research and Development program for support. Sandia is a multiprogram laboratory operated by Sandia Corporation, a Lockheed Martin Company, for the United States Department of Energy's National Nuclear Security Administration under Contract DE-AC04-94AL85000.

Notes and references

1 D. E. Discher, P. Janmey and Y. Wang, *Science*, 2005, **310**, 1139.
2 M. H. Zaman, L. M. Trapani, A. L. Sieminski, D. MacKellar, H. Gong, R. D. Kamm, A. Wells, D. A. Lauffenburger and P. Matsudaira, *Proc. Natl. Acad. Sci. U. S. A.*, 2006, **103**, 10889.
3 D. P. McDaniel, G. A. Shaw, J. T. Elliott, K. Bhadriraju, C. Meuse, K. H. Chung and A. L. Plant, *Biophys. J.*, 2007, **92**, 1759–1769.
4 T. Boontheekul, E. E. Hill, H. J. Kong and D. J. Mooney, *Tissue Eng.*, 2007, **13**, 1431–1442.
5 M. J. Paszek, N. Zahir, K. R. Johnson, J. N. Lakins, G. I. Rozenberg, A. Gefen, C. A. Reinhart-King, S. S. Margulies, M. Dembo and D. Boettiger, *Cancer Cell*, 2005, **8**, 241–254.
6 S. Akizuki, V. C. Mow, F. Müller, J. C. Pita, D. S. Howell and D. H. Manicourt, *J. Orthop. Res.*, 1986, **4**, 379–392.
7 S. Park and G. A. Ateshian, *J. Biomech. Eng.*, 2006, **128**, 623.
8 V. C. Mow, M. C. Gibbs, W. M. Lai, W. B. Zhu and K. A. Athanasiou, *J. Biomech.*, 1989, **22**, 853.
9 J. A. Last, S. J. Liliensiek, P. F. Nealey and C. J. Murphy, *J. Struct. Biol.*, 2009, **167**, 19–24.
10 S. S. Soofi, J. A. Last, S. J. Liliensiek, P. F. Nealey and C. J. Murphy, *J. Struct. Biol.*, 2009, **167**, 216–219.
11 L. Almany and D. Seliktar, *Biomaterials*, 2005, **26**, 2467–2477.
12 J. El-Ali, P. K. Sorger and K. F. Jensen, *Nature*, 2006, **442**, 403.
13 D. B. Weibel, W. R. Diluzio and G. M. Whitesides, *Nat. Rev. Microbiol.*, 2007, **5**, 209–218.
14 C. N. LaFratta, J. T. Fourkas, T. Baldacchini and R. A. Farrer, *Angew. Chem., Int. Ed.*, 2007, **46**, 6238–6258.
15 B. Kaehr, R. Allen, D. J. Javier, J. Currie and J. B. Shear, *Proc. Natl. Acad. Sci. U. S. A.*, 2004, **101**, 16104.
16 B. Kaehr and J. B. Shear, *J. Am. Chem. Soc.*, 2007, **129**, 1904–1905.
17 B. Kaehr and J. B. Shear, *Proc. Natl. Acad. Sci. U. S. A.*, 2008, **105**, 8850.
18 B. Kaehr and J. B. Shear, *Lab Chip*, 2009, **9**, 2632–2637.
19 R. Nielson, B. Kaehr and J. B. Shear, *Small*, 2009, **5**, 120.
20 S. K. Seidlits, C. E. Schmidt and J. B. Shear, *Adv. Funct. Mater.*, 2009, **19**, 3543–3551.
21 A. J. Poole, J. S. Church and M. G. Huson, *Biomacromolecules*, 2008, **10**, 1–8.
22 O. Okay and S. Durmaz, *Polymer*, 2002, **43**, 1215–1221.
23 D. F. Young, W. F. Riley, K. G. McConnell and T. R. Rogge, *Essentials of Mechanics: A Unified First Course*, Wiley-Blackwell, 1974.
24 Z. Bayindir, Y. Sun, M. J. Naughton, C. N. LaFratta, T. Baldacchini, J. T. Fourkas, J. Stewart, B. E. A. Saleh and M. C. Teich, *Appl. Phys. Lett.*, 2005, **86**, 064105.
25 J. B. Matthew and F. R. Gurd, *Methods Enzymol.*, 1986, **130**, 413.
26 R. K. Scopes, *Protein Purification: Principles and Practice*, Springer-Verlag, 1994.
27 N. M. Green, *Adv. Protein Chem.*, 1975, **29**, 85.
28 D. Malamud and J. W. Drysdale, *Anal. Biochem.*, 1978, **86**, 620–647.
29 W. J. Leonard, Jr and J. F. Foster, *J. Biol. Chem.*, 1961, **236**, 2662.
30 P. Relkin, *Crit. Rev. Food Sci. Nutr.*, 1996, **36**, 565–601.
31 M. Yamasaki, H. Yano and K. Aoki, *Int. J. Biol. Macromol.*, 1990, **12**, 263.
32 K. Ogasahara and K. Hamaguchi, *J. Biochem.*, 1967, **61**, 199.
33 N. N. Khechinashvili, P. L. Privalov and E. I. Tiktopulo, *FEBS Lett.*, 1973, **30**, 57–60.
34 N. M. Green, *Biochem. J.*, 1963, **89**, 609.
35 T. Kosa, T. Maruyama and M. Otagiri, *Pharm. Res.*, 1998, **15**, 449–454.
36 J. C. Bischof and X. He, *Ann. N. Y. Acad. Sci.*, 2005, **1066**, 12.
37 A. Michnik, *J. Therm. Anal. Calorim.*, 2003, **71**, 509–519.
38 M. González, C. E. Argaraña and G. D. Fidelio, *Biomol. Eng.*, 1999, **16**, 67–72.
39 F. Ismoyo, Y. Wang and A. Ismail, *Appl. Spectrosc.*, 2000, **54**, 939–947.
40 J. J. Vlassak and W. D. Nix, *J. Mater. Res.*, 1992, **7**, 3242–3249.
41 M. Stohrer, Y. Boucher, M. Stangassinger and R. K. Jain, *Cancer Res.*, 2000, **60**, 4251.
42 E. S. Benson, B. E. Hallaway and R. W. Lumry, *J. Biol. Chem.*, 1964, **239**, 122–129.

